

# Wind noise at microphones within and across hearing aids at wind speeds below and above microphone saturation<sup>a)</sup>

Justin A. Zakis<sup>b)</sup>

*Dynamic Hearing Pty Ltd., 2 Chapel Street, Richmond, Victoria 3121, Australia*

(Received 7 December 2010; revised 21 March 2011; accepted 23 March 2011)

The variation of wind noise at hearing-aid microphones with wind speed, wind azimuth, and hearing-aid style was investigated. Comparisons were made across behind-the-ear (BTE) and completely-in-canal (CIC) devices, and between microphones within BTE devices. One CIC device and two BTE devices were placed on a Knowles Electronics Manikin for Acoustic Research. The smaller BTE device had vented plastic windshields around its microphone ports while the larger BTE device had none. The microphone output signals were digitally recorded in wind generated at 0, 3, 6, and 12 m/s at 8 wind azimuths. The microphone output signals were saturated at 12 m/s with wind-noise levels of up to 116 dB SPL at the microphone output. Wind-noise levels differed by up to 12 dB between microphones within the same BTE device, and across BTE devices by up to 6 or 8 dB for front or rear microphones, respectively. On average, wind-noise levels were lowest with the CIC device and highest at the rear microphone of the smaller BTE device. Engineering and clinical implications are discussed. © 2011 Acoustical Society of America. [DOI: 10.1121/1.3578453]

PACS number(s): 43.66.Ts, 43.50.Yw, 43.28.Vd, 43.38.Kb [BLM]

Pages: 3897–3907

## I. INTRODUCTION

Hearing aids can be exposed to environmental wind and other air flows, such as those generated by fans or from walking, jogging, or riding a bicycle. Pressure variations from turbulence in such air flows results in what is often referred to as wind noise in the microphone's output signal. Wind noise is a serious problem with hearing aids. Although satisfaction with hearing aids in wind noise has recently increased by 7% over 4 years (Kochkin, 2010), 58% of users of recent devices (no greater than 4 years old) have various degrees of satisfaction for wind noise, while 20% are neither satisfied nor dissatisfied, and 22% have various degrees of dissatisfaction (Kochkin, 2010). Satisfaction for wind noise (total satisfied = 58%) was lower than for any of the 10 other items in the "Signal processing and sound quality" category of Kochkin (2010) including "Use in noisy situations" (total satisfied = 61%).

In comparison, recent hearing aids can perform much more satisfactorily in listening situations such as "One-on-one" (total satisfied = 91%) and "Small groups" (total satisfied = 85%) (Kochkin, 2010). The relatively low satisfaction for wind noise is important, because overall satisfaction with hearing-aid benefit increases with the percentage of the 19 surveyed listening situations in which aid users are satisfied (Kochkin, 2010) and wind noise may be present in several of these situations. However, despite the continuing problem of wind noise with hearing aids, it has attracted comparatively little attention in the literature. A better acoustical understanding of wind noise could better inform

the design of future hearing-aid hardware and signal-processing algorithms to increase satisfaction in wind noise.

For conciseness, throughout this paper an air flow generated by a wind tunnel is simply referred to as "wind," and the signal the wind generates at the microphone output is referred to as "wind noise." It is well established that wind noise can be greater at the output of a directional microphone than an omni-directional microphone (Beard and Nepomuceno, 2001; Thompson and Dillon, 2002; Chung *et al.*, 2009, 2010). The long-term-average, wind-noise spectrum can vary with wind azimuth (horizontal plane), style of hearing aid, and/or hearing-aid shell design for a particular hearing-aid style (Dillon *et al.*, 1999, 2000; Grenner *et al.*, 2000; Beard and Nepomuceno, 2001; Thompson and Dillon, 2002; Chung *et al.*, 2009, 2010). Some studies have also shown that wind-noise levels increase with wind speed (Beard and Nepomuceno, 2001; Chung *et al.*, 2009, 2010).

However, most previous studies reported wind-noise levels measured at the microphone for one or two relatively low wind speeds of up to 5 m/s (Dillon *et al.*, 1999; 2000; Beard and Nepomuceno, 2001; Thompson and Dillon, 2002) or at the hearing-aid output at 7 m/s (Grenner *et al.*, 2000). A wind speed of 5 m/s, which is 18.0 km/h, 11.2 mph, or 9.7 knots, corresponds to a rating of 3 (gentle breeze) on the 13-point Beaufort wind force scale, and hearing-aid users could encounter stronger winds in everyday life. Few studies have investigated wind noise at higher wind speeds, where wind-noise levels at the microphone output would increase up to the microphone's saturation point, and have greater potential to mask speech and risk loudness discomfort. Saturation of the microphone signal would also lead to clipping distortion of speech and other important sounds embedded in the wind noise, which would result in the generation of high-frequency harmonics. Thus, it is important that the wind speeds that can cause microphone saturation and its consequences are better understood.

<sup>a)</sup>Portions of this work were presented in "An analysis of wind noise at the front and rear microphones of hearing aids," poster presented at The International Hearing-Aid Conference 2010, Lake Tahoe, CA, USA, 11–15 August 2010.

<sup>b)</sup>Author to whom correspondence should be addressed. Electronic mail: jzakis@dynamichearing.com.au

The author is aware of two studies that used higher wind speeds, where hearing aids were fitted to a Knowles Electronics Manikin for Acoustic Research (KEMAR) (Burkhard and Sachs, 1975) and wind-noise levels were measured at the ear drum for wind speeds at multiples of 4.5 m/s up to 13.5 (Chung *et al.*, 2010) or 22.5 m/s (Chung *et al.*, 2009). The fitted, linear gain was used to derive wind-noise input levels for the 125, 500, and 2000 Hz one-third-octave bands and the total wideband level across all bands. However, the aids had input or output limiters that could not be turned off, which could result in similar measured output levels (and hence estimated wind-noise input levels) for wind speeds of 9.0 and 13.5 m/s at some wind azimuths. Thus, the literature does not clearly show wind-noise spectra at the microphone output for wind speeds greater than 5–7 m/s, the wind speeds at which microphone saturation can occur, or the corresponding wind-noise levels at microphone saturation.

Behind-the-ear (BTE) styles of hearing aid often have two omni-directional microphones, while the aforementioned studies reported wind-noise levels at one omni-directional or directional microphone per BTE device. Hearing aids often switch from a directional microphone to the front omni-directional microphone in wind (Chung, 2004), since wind-noise levels are typically lower with an omni-directional microphone (Beard and Nepomuceno, 2001; Chung *et al.*, 2009, 2010). However, it is not clear whether further reductions in wind-noise levels can be achieved by switching between the front and rear omni-directional microphones, and whether this depends on the wind speed, wind azimuth, or hearing-aid shell design. If such switching reduced wind-noise levels at the hearing-aid input, it could reduce the likelihood of a clipped (distorted) microphone output signal and increase the speech-to-wind-noise ratio before digital signal processing. This in turn could increase listening comfort, reduce the dependence on wind-noise reduction algorithms, and thereby lead to improved satisfaction with hearing aids in wind noise.

This paper presents an investigation into the variation of one-third-octave band and wideband wind-noise levels with hearing-aid style, BTE device shell, microphone location within a BTE shell (i.e., front versus rear), wind azimuth, and wind speed below and above microphone saturation (0, 3, 6, and 12 m/s). Two dual-microphone, BTE devices and one single-microphone, completely-in-canal (CIC) device were used. The microphone ports of the large BTE device (BTE1) had no mechanical wind shields, while the microphone ports of the smaller BTE device (BTE2) were partially covered by vented, plastic wind shields. Cables were soldered to the microphone output terminals, and stereo (i.e., front and rear) digital recordings of the omni-directional microphone signals were made for each combination of wind azimuth, wind speed, and device. The recordings were analyzed to calculate the long-term-average, one-third-octave, wind-noise spectrum and the wideband wind-noise level across all one-third-octave bands at each microphone. The wind-noise levels were compared between microphones within each BTE device and between microphones across all devices, as well as with the long-term-average speech spectrum to estimate the possible speech-to-wind noise ratio.

## II. METHODS

### A. Hearing-aid hardware

Two dual-microphone, BTE shells and a single-microphone CIC device were used. All devices contained Knowles FG-series, cylindrical, omni-directional microphones and no other electronic circuits. These microphones had a nominally flat frequency response from 100 Hz to 10 kHz, a nominal sensitivity of  $-53$  dBV/0.1 Pa, and a typical, input-referred, self-noise level of 27 dB(A) (1 kHz reference). The power, signal, and ground terminals of each microphone were soldered to a shielded, three-conductor cable. The cables exited from the bottom of each BTE device, and from the eardrum-facing side of the CIC device (i.e., into the KEMAR's head and down out of its neck).

Figure 1 shows line diagrams of the BTE devices (microphones are shown in grey) and a photograph of the CIC device. BTE1 was a large device (size 675 battery) that had no mechanical wind protection around its microphone ports. BTE2 was a medium-sized device (size 13 battery) with its front microphone port opening into an earhook cavity that had horizontal vents, and its rear microphone port was covered by a small, rearward-facing, half dome. The CIC device was an ER-14B, expandable-foam, insert earphone tip, which had a rigid plastic tube running through its center. A cylindrical microphone was securely placed in this tube with its inlet port flush with the external surface of the foam plug.

### B. Wind-noise recording apparatus

Figure 2 shows an overhead diagram of the low-noise wind source at the National Acoustic Laboratories (Chatswood, NSW, Australia) that was used for this study. Fine details of its design and construction are available in Fishburn *et al.* (2007). Air flow was generated by an 18.5-kW, variable-speed, centrifugal fan, which was housed at one end of a concrete tube (shown across the top of Figure 2) that had 200-mm thick walls and a rectangular cross sectional area of  $4$  m<sup>2</sup>. The air flow passed between three parallel baffles (each 5 m long, 2 m high, and 250 mm thick) that formed a silencer (shown on right of fan in Figure 2) that reduced the fan noise

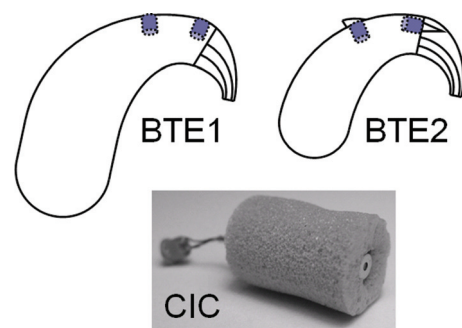


FIG. 1. (Color online) Diagrams of the ear-level devices used in this study. Each device contained one or two microphones and no other circuits. BTE1 was a large device with unshielded microphone ports. BTE2 was a medium-size device with mechanical wind shielding around the microphone ports. CIC was a foam earplug with a microphone securely located in its sound bore. Shielded cables connected the microphone output signals to the digital recording equipment and provided power and ground connections for the microphones.

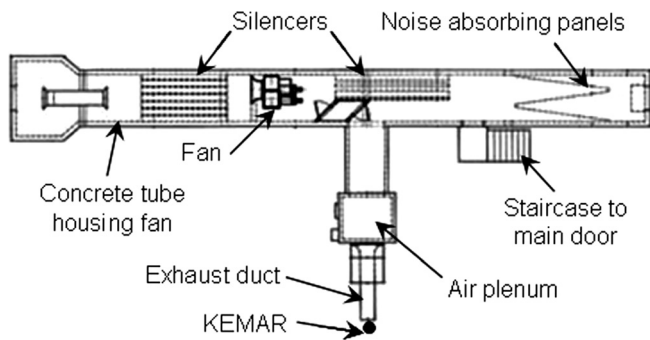


FIG. 2. Overhead diagram showing the wind generator and location of the KEMAR head. Schematic provided by the National Acoustic Laboratories, Chatswood, Australia (labels, arrows and KEMAR added).

by 56 dB(Lin.). The air flow turned 180° between this silencer and additional sound-absorbing panels, and then 90° to exit the concrete tube and enter a smaller duct via a smooth cross-sectional area transition region. The air flow exited this duct and into the top of a 12 m<sup>3</sup> air plenum that stabilized the air flow. The air flow exited from the bottom of the plenum into a smooth transition duct (transition area ratio of 5:1), which further stabilized the air flow before entering the straight, metal, exhaust duct that had a square 61 × 61 cm outlet. The fan noise exiting the exhaust duct was reported as 41 and 63 dB(A) for flows of 2700 l/s (7.3 m/s) and 4300 l/s (11.6 m/s), respectively (Fishburn *et al.*, 2007).

The fan speed was controlled via a digital variable frequency controller across a 0–50 Hz range with a resolution of 0.1 Hz. The air flow was approximately 8000 l/s at full fan speed. The wind speed at the exhaust outlet was measured with a mini-vane digital anemometer (Lutron LM-81AM: 3% accuracy, 0.1 m/s resolution) and confirmed with another (DSE Q1301: 0.1 m/s resolution) and the fan speed was adjusted to give wind speeds of 3, 6, and 12 m/s. Entering the corresponding fan speed (i.e., frequency) values into the digital controller gave repeatable wind speed measurements.

A KEMAR head was placed on a length of pipe that acted as a neck and had its base attached to a turntable. The center of the KEMAR head was positioned in the center of the wind stream and 20 cm from the end of the wind generator's 61 × 61 cm outlet (the turntable was below the outlet and out of the wind stream). The ear-level devices were placed on the right ear, and the ear canal was removed so the cable from the CIC device could exit down the inside of the neck. The shielded cables of the BTE devices were securely taped to the neck to avoid wind-induced vibration noise. The cables connected the microphones to the input and ground of an Echo Indigo, external, 32-bit, stereo sound card (dynamic range > 109 dB(A), frequency response 10-20,000 Hz, ±0.5 dB) and a 1.5-volt, AA-size cell to power the microphones. Adobe Audition 1.5 software was configured to make 32-bit, stereo recordings of the microphone signal(s) of each device with a 44.1-kHz sampling rate.

### C. Wind-noise recording procedure

Throughout this paper, the wind azimuth (i.e., the spatial origin of the wind on the horizontal plane) will be defined as

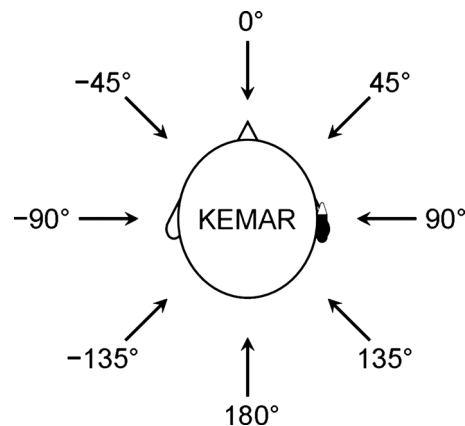


FIG. 3. Overhead diagram showing the tested wind azimuths relative to the KEMAR wearing an ear-level device on its right ear.

follows: 0° is for wind from directly in front of the head; +90° is for wind from the (right) side of the head that has the hearing aid (i.e., aid facing upstream); -90° is for wind from the (left) side of the head that does not have the hearing aid (i.e., aid facing downstream); and 180° is for wind from directly behind the head. Figure 3 shows the direction of the wind relative to the KEMAR head for the eight tested azimuths.

One ear-level device was located on the KEMAR head at any one time. Recordings of the microphone output signals were first made for BTE1, followed by BTE2 and then the CIC device so that each device remained in the same position for all of its recordings. Recordings were made at wind speeds of 0, 3, 6, and then 12 m/s. For each wind speed, the head was initially positioned to face the wind outlet (0° azimuth) and then rotated in 45° increments. Each wind-noise recording was 10 seconds long, and a total of 96 stereo recordings were made (3 devices × 4 wind speeds × 8 azimuths). The wind-noise recordings were saved as 32-bit WAV files for post-processing and analysis.

### D. Calibration measurements and post-processing

Additional 10 s recordings were made with each device placed in a Brüel & Kjær Type 4232 anechoic test box and presented with white noise at 80 dB SPL(Linear) (44.1 kHz sampling rate). These recordings encapsulated the sensitivity of each microphone across frequency and were later used to calibrate the wind-noise recordings in dB SPL (re: 20 μPa) units. White noise was used because it has a flat spectrum with the linearly spaced frequency bands that were used to calibrate the wind-noise levels for the microphone prior to conversion to one-third-octave bands. The white-noise input stimulus file and all microphone recordings for both the wind- and white-noise stimuli were then anti-aliasing filtered and down sampled from 44.1 to 20 kHz in Adobe Audition 1.5. This made all files match the nominal 10-kHz bandwidth of the anechoic test box used for the microphone calibration recordings (nominal flat frequency response ±3dB from 35 Hz to 10 kHz, -24 dB/octave roll off above 10 kHz), and share the same anti-aliasing filter roll-off below the Nyquist frequency of 10 kHz. The 20-kHz sampling rate was also

chosen because it was similar to rates used by commercial hearing aids, and allowed the analysis of the entire 8-kHz one-third-octave band. The down sampled white-noise input stimulus was presented in the anechoic test box, and its wideband level of 79 dB SPL was noted as the reference input level for the down sampled, white-noise, microphone calibration recordings.

The down-sampled, white-noise, microphone calibration recordings had the combined frequency response of the microphones and the anechoic test box that presented the white-noise input stimulus. In order to measure the test box response, a Brüel & Kjær Type 4189 microphone (flat frequency response  $\pm 0.5$  dB from 20–10,000 Hz) was placed in the test box and connected to a Brüel & Kjær Type 2260 sound level meter via the box's external electrical terminal. The down sampled, white-noise, input stimulus was presented at 79 dB SPL, and the one-third-octave band levels were measured from 20–10,000 Hz. The following section describes how these levels and the white-noise microphone calibration recordings were used to calibrate the wind-noise recordings in dB SPL.

### E. Wind-noise analysis

A custom MATLAB® (R2008b) script performed spectral analysis on the down sampled, white-noise, input stimulus file and all down sampled white- and wind-noise recordings. Analysis was performed from 0.5 to 9.5 s into each 10 s file to avoid possible transients at the start and end of the recordings. Frames of 16,384 samples were processed with a 16,384-point Hanning window and Fast Fourier Transform (FFT) with 75% temporal overlap between FFT frames (i.e., a window hop of 4096 samples). The resulting spectral estimates consisted of 8192 FFT bins with center frequencies linearly spaced at multiples of 1.22 Hz from 0 to 9999 Hz. The wind-noise spectrum for each microphone was calculated in dB SPL units for each frame of each wind-noise recording with Eq. (1).

$$\mathbf{XdBSPL}_{bn} = 20 \log_{10}(|\mathbf{X}_{bn}| + \text{eps}) + 39.866 - \mathbf{CalRecdB}_b \quad (1)$$

where  $\mathbf{XdBSPL}$  is a matrix of wind-noise levels in dB SPL,  $b = \{1, \dots, 8192\}$  is the FFT bin number (0 Hz and positive frequencies),  $n = \{1, \dots, 44\}$  is the FFT frame number,  $\mathbf{X}$  is a matrix of complex FFT data for the relevant microphone and wind-noise recording, eps is the smallest numerical value in MATLAB (2.2204e-16), 39.866 is the expected input level (dB SPL units) for each FFT bin for white noise presented at 79 dB SPL, and  $\mathbf{CalRecdB}$  is the recorded input level in numerical dB units (re: 1.0) for each FFT bin calculated from the white-noise calibration recording for the same microphone. Thus, for each FFT bin and frame, the wind-noise level was calculated in numerical dB units (re: 1.0) from the magnitude of the complex FFT data, and was converted to dB SPL units by adding the difference between the expected SPL at the microphone input (39.866 dB SPL) and the measured numerical dB level (re: 1.0) at the microphone output ( $\mathbf{CalRecdB}$ ) for white noise presented at 79 dB SPL.

The  $\mathbf{CalRecdB}$  values were calculated from the relevant white-noise microphone calibration recording with Eq. (2).

$$\mathbf{CalRecdB}_b = 20 \log_{10} \left( \sqrt{\frac{\sum_{n=1}^N |\mathbf{Y}_{bn}|^2}{N}} \right) + \mathbf{CalRippledB}_b \quad (2)$$

where  $\mathbf{Y}$  is a matrix of complex FFT data for the white-noise microphone calibration recording,  $N$  is the total number of FFT frames, and  $\mathbf{CalRippledB}$  is a vector of spectral ripple compensation data in numerical dB units (re: 1.0) for the white-noise input stimulus file. Thus, the power for each FFT bin was averaged across FFT frames and converted to numerical dB units (re: 1.0) for the relevant white-noise microphone calibration recording. These long-term-average values were adjusted by  $\mathbf{CalRippledB}$  to compensate for ripples in the long-term-average spectrum of the white-noise input stimulus, which appeared in the long-term-average spectra of the white-noise microphone calibration recordings. Spectral ripples of up to approximately  $\pm 3$  dB were evident because of the analysis of a random noise over a non-infinite averaging time with very fine frequency resolution (16,384-point FFT). Equations (3) and (4) show how  $\mathbf{CalRippledB}$  was calculated from the white-noise input stimulus file.

$$\mathbf{CalRippledB}_b = \frac{\sum_{b=1}^{7936} \mathbf{CalInputdB}_b}{7936} - \mathbf{CalInputdB}_b, \quad (3)$$

$$\mathbf{CalInputdB}_b = 20 \log_{10} \left( \sqrt{\frac{\sum_{n=1}^N |\mathbf{Z}_{bn}|^2}{N}} \right), \quad (4)$$

where  $\mathbf{Z}$  is a matrix of complex FFT data for the white-noise input stimulus file, and  $\mathbf{CalInputdB}$  is a corresponding vector of long-term-average, numerical levels for the FFT bins in dB units (re: 1.0). Thus, the ripple compensation value for each bin was its long-term-average level in dB units subtracted from the mean dB level across the lowest 7936 (i.e.,  $8192 \times 31/32$ ) FFT bins centered from 0 to 9685 Hz. The mean dB level was calculated across bins that were not affected by anti-aliasing filter roll-off, which was above the upper boundary of the greatest one-third-octave band of interest (centered at 8 kHz). The resultant  $\mathbf{CalRippledB}$  vector had a zero mean across these bins.

The processing described above estimated the wind-noise level in dB SPL units for each FFT bin and frame ( $\mathbf{XdBSPL}$ ), but did not take into account the frequency response of the test box used to make the white-noise, microphone calibration recordings. This was done through the calculation of long-term-average, one-third-octave, wind-noise levels from  $\mathbf{XdBSPL}$  with Eq. (5) and (6).

$$\mathbf{Xpower}_{bn} = 10^{\mathbf{XdBSPL}_{bn}/10}, \quad (5)$$

$$\mathbf{XdBSPL}_{Oct,d} = 10 \log_{10} \left( \sum_{b=i}^j \sum_{n=1}^N \frac{\mathbf{Xpower}_{bn}}{N} \right) - \mathbf{BoxCompdB}_d, \quad (6)$$

where  $\mathbf{Xpower}$  is a matrix of wind-noise power values for each FFT bin and frame,  $\mathbf{XdBSPLoct}$  is a matrix of corresponding long-term-average, one-third-octave, wind-noise levels in dB SPL,  $d$  is the one-third-octave band number,  $i$  is the number of the lowest FFT bin in band  $d$ ,  $j$  is the number of the highest FFT bin in band  $d$ , and  $\mathbf{BoxCompdB}$  is a vector of compensation data for the frequency response of the anechoic test box used to make the white-noise microphone calibration recordings. Thus, the wind-noise FFT spectra were converted from dB SPL to power units in Eq. (5), and the long-term-average power was calculated for each FFT bin and summed across FFT bins in each one-third-octave band, and then converted back to dB SPL units in Eq. (6). The test-box compensation data ( $\mathbf{BoxCompdB}$ ) were the expected one-third-octave levels for white noise presented at 79 dB SPL minus the levels previously measured in the anechoic test box. The MATLAB script stored the  $\mathbf{XdBSPLoct}$  values for one-third-octave bands centered from 63 to 8000 Hz for different microphones and wind-noise recordings into text files. Lower bands were not included because the white-noise microphone calibration recordings were affected by 50-Hz mains supply noise. The upper limit of the 8 kHz band (8980 Hz) was not affected by anti-aliasing filter roll-off.

### III. RESULTS

#### A. Wind-noise level spectra

Figures 4, 5, and 6 show the long-term-average, one-third-octave, wind-noise spectra for all microphones and azimuths at wind speeds of 3, 6, and 12 m/s, respectively. Each graph shows a different azimuth, and are arranged so that their positions correspond to the wind directions as shown in Figure 3 (except for 180°). The circles, squares, and plus symbols correspond to BTE1, BTE2, and the CIC device, respectively. Filled and open symbols correspond to front and rear microphones for the BTE devices, respectively. The thick solid line shows the non-wind, noise-floor level, which was calculated by adding (in power units) the long-term-average SPL from the 0 m/s recordings (averaged across azimuths and devices), and the SPL of the noise exiting the wind generator outlet as reported by Fishburn *et al.* (2007) after conversion from octave to one-third-octave levels. The data of Fishburn *et al.* (2007) for 7.3 and 11.6 m/s were used for the 6 and 12 m/s graphs, respectively. These were the closest wind speeds reported by Fishburn *et al.* (2007) to those used in the current study (lower non-zero wind speeds were not reported). Although not exact, the 3 m/s outlet noise data were simply estimated via linear extrapolation (in dB units), since there was an approximately linear relationship between wind speed and the outlet noise reported at 7.3, 11.6, and 15.3 m/s by Fishburn *et al.* (2007). As a speech reference, the thin solid and dashed lines show the 65 dB SPL long-term-average speech spectrum (LTASS) at the BTE and CIC microphone locations, respectively. The LTASS curves were derived by subtracting 5 dB from combined (male and female) 70 dB SPL LTASS of Byrne *et al.* (1994), and adding the free-field to BTE or CIC microphone position transformation data of Dillon (2001) (page 93, Table IV.5, talker at 0° azimuth).

Figure 4 shows that at 3 m/s, the band levels were below 80 dB SPL for all devices and azimuths. The wind-noise level tended to exceed the LTASS in the lower frequencies. This occurred over the smallest range of bands at 90° azimuth, where the wind noise exceeded the LTASS below 100 Hz with the CIC and below 125–200 Hz with the BTE microphones. The wind noise dominated the LTASS over the greatest number of bands at 0° azimuth, ranging from below the 315-Hz band for the CIC device, and below the 1.6-kHz band for the front microphone of BTE1. For the rear BTE microphones, the wind noise exceeded the LTASS over the greatest number of bands at 180° with a worst case of below 1.6 kHz for BTE2. For the BTE devices, one-third-octave, wind-noise levels tended to be most clearly greater at the front microphones at 0° and –45°, and at the rear microphones at 180° and –135°. The band levels at the CIC microphone were generally comparable to the lower BTE levels, and were most clearly lower than the BTE levels at 180° and greater at 135°.

Figure 5 shows a similar pattern of results at 6 m/s with some notable differences. Wind-noise levels exceeded 90 dB SPL in some bands, and the increase in level was greater at high than low frequencies. At 90° azimuth, the LTASS was exceeded below the 200-Hz band for the CIC device and below 500–2000 Hz for the BTE devices. The LTASS was exceeded over the greatest number of bands at 0° for the front BTE microphones (below 6.3 kHz), at 180° for the rear BTE microphones (below 8 kHz for BTE1, and up to 8 kHz for BTE2), and at 135° for the CIC device (below 6.3 kHz). At 6 m/s, wind-noise levels tended to be most clearly lower with the CIC device at most azimuths, while at 135° wind-noise levels were not always clearly higher with the CIC device and were more comparable to levels with the BTE devices.

Figure 6 shows that at 12 m/s, wind-noise spectra tended to flatten with band levels as high as 109 dB SPL (BTE2, rear microphone, –90°). Inspection of the waveforms in the recordings suggests that the microphone output had saturated (clipped) for all devices and azimuths (note: this was approximately 15 dB below the input clipping level of the sound card). Wind-noise levels were most clearly higher with the rear BTE microphones at –135°, 180°, and 45°, and most clearly lowest at the CIC microphone at 90° and 180°. The wind-noise level exceeded the LTASS in all bands for all microphones and azimuths.

#### B. Wideband wind-noise levels

Figure 7 shows the wideband wind-noise levels plotted against azimuth for 3 m/s (bottom plots), 6 m/s (middle plots) and 12 m/s (top plots). The allocation of symbols to microphones is the same as for the one-third-octave spectra shown in Figs. 4–6. Solid lines connect points for BTE1, dashed lines for BTE2, and dotted lines for the CIC device. The symbols to the right of the 180° point show the mean across all azimuths for each microphone at each wind speed. At lower wind speeds, wideband wind-noise levels tended to peak around –45 to 0° for all devices, with another peak around –135 and 180° for the BTE devices and 135° for the

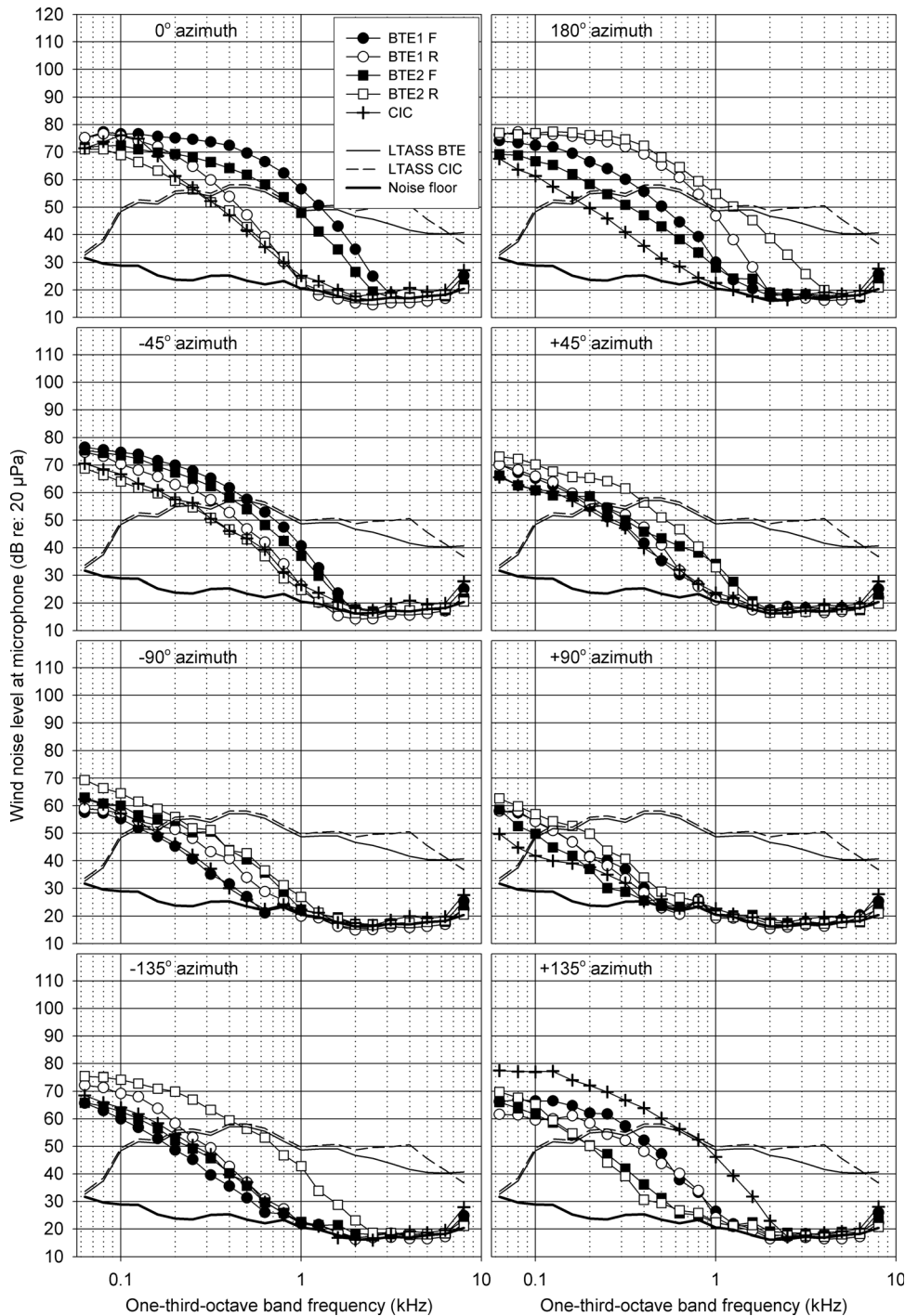


FIG. 4. Long-term average, one-third-octave, wind-noise spectra at the microphones for each azimuth and a wind speed of 3 m/s. For comparison, the estimated non-wind noise floor (thick lines) and the long-term average speech spectrum (65 dB SPL) at the typical BTE (solid thin lines) and CIC (dashed thin lines) microphone locations for a talker at 0° azimuth are also shown.

CIC device. The lowest levels tended to be at 90° (i.e., aid upstream of head), with a shallower valley at -90° (i.e., aid downstream of head) for 3 and 6 m/s, but not 12 m/s. Wind-noise levels varied with azimuth over a smaller range of levels at higher than at lower wind speeds. The lowest wideband level was 52 dB SPL at the CIC microphone for 3 m/s at 90°, and the highest was 116 dB SPL at the rear microphone of BTE2 for 12 m/s at -90°, 45°, and 180°.

### C. Within-BTE device wideband level differences

Figure 8 (left graphs) shows the wideband wind-noise level at the rear microphone relative to the front microphone

of each BTE device for 3, 6 and 12 m/s. Thus, positive values show greater levels at the rear than the front microphone of a particular BTE device. Differences are shown with hexagons and solid lines for BTE1, and with diamonds and dashed lines for BTE2. The values to the far right show the average differences across azimuth, which were 0–1 dB for BTE1 and 4–6 dB for BTE2.

Differences across azimuths tended to be greater in magnitude for BTE2 than BTE1, and smaller at higher wind speeds for both BTE devices. Positive differences (i.e., rear microphone level greater) tended to be greatest around -135° and 180° for both devices (up to 8 dB for BTE1 and 12 dB for BTE2 at 3 m/s) with another prominent peak at 45° for BTE2

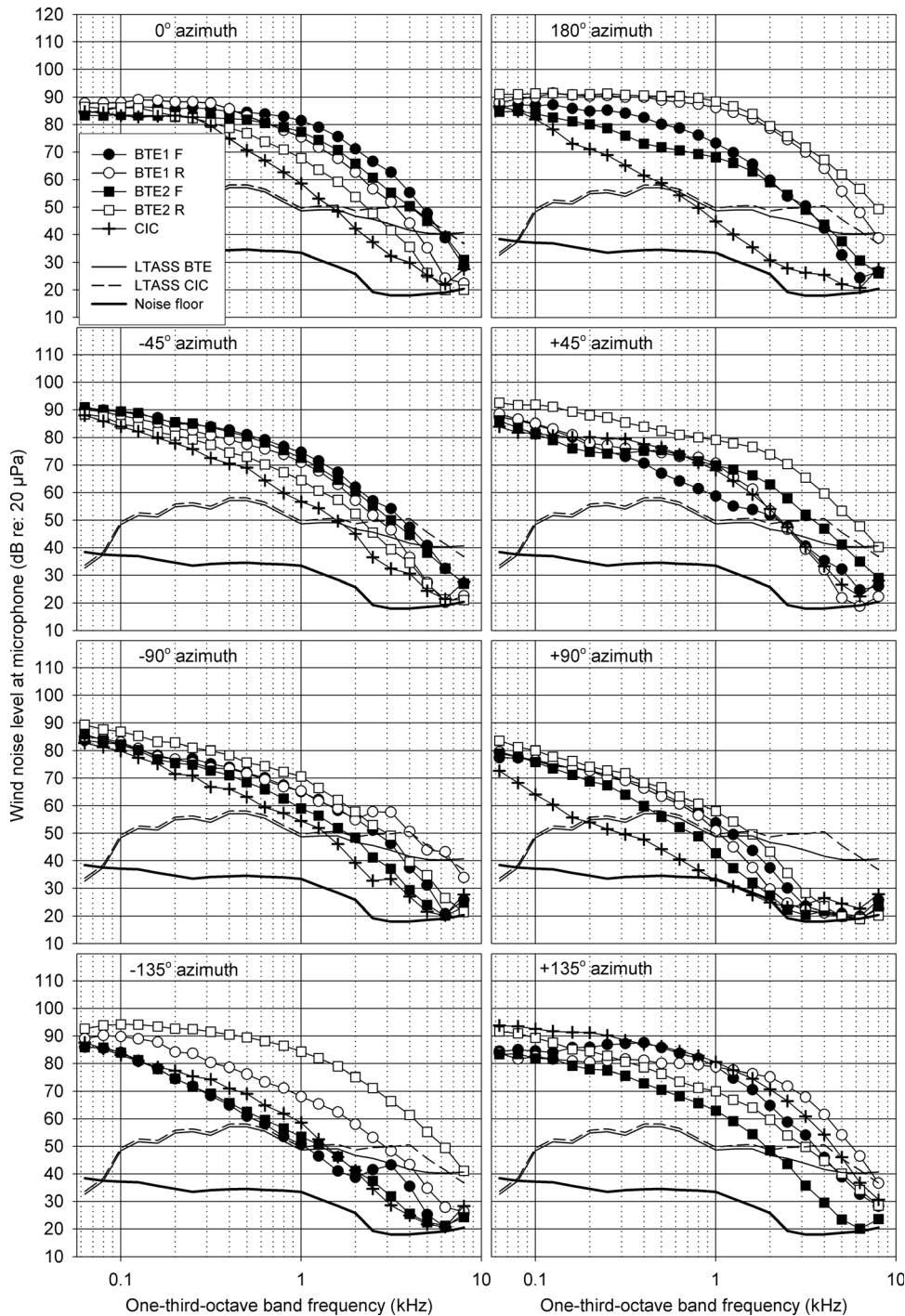


FIG. 5. As for Figure 4, except for a wind speed of 6 m/s.

but not BTE1 (where differences were close to zero). Negative differences (i.e., rear microphone level lower) tended to be greatest around  $-45^\circ$  for both BTE devices (as great as  $-8$  dB for BTE2 at 3 m/s), and also at  $135^\circ$  for BTE1 at lower wind speeds (as great as  $-5$  dB at 3 m/s) but not BTE2 (where differences were positive).

#### D. Across-device wideband level differences

Figure 8 (right graphs) shows differences in wideband, wind-noise levels across devices for 3, 6, and 12 m/s. All differences are relative to BTE1, so positive differences show greater levels at the comparison devices. Differences are

shown for BTE2 relative to BTE1 for their front (filled triangles) and rear (open triangles) microphones, and for the CIC microphone relative to the front microphone of BTE1 (plus symbols and dashed lines). The values to the far right show the averages across azimuth.

Differences between devices tended to vary less across azimuth with increasing wind speed. Comparing the front microphones of the BTE devices, differences tended to be maximally positive (i.e., BTE2 level higher) around  $-90^\circ$  (up to 5 dB at 3 m/s) and tended to be negative (i.e., BTE2 level lower) across a range of azimuths that were mainly on the hearing-aid side (i.e., positive azimuths) and were as great as  $-6$  dB at 6 m/s. In contrast, for the rear microphones

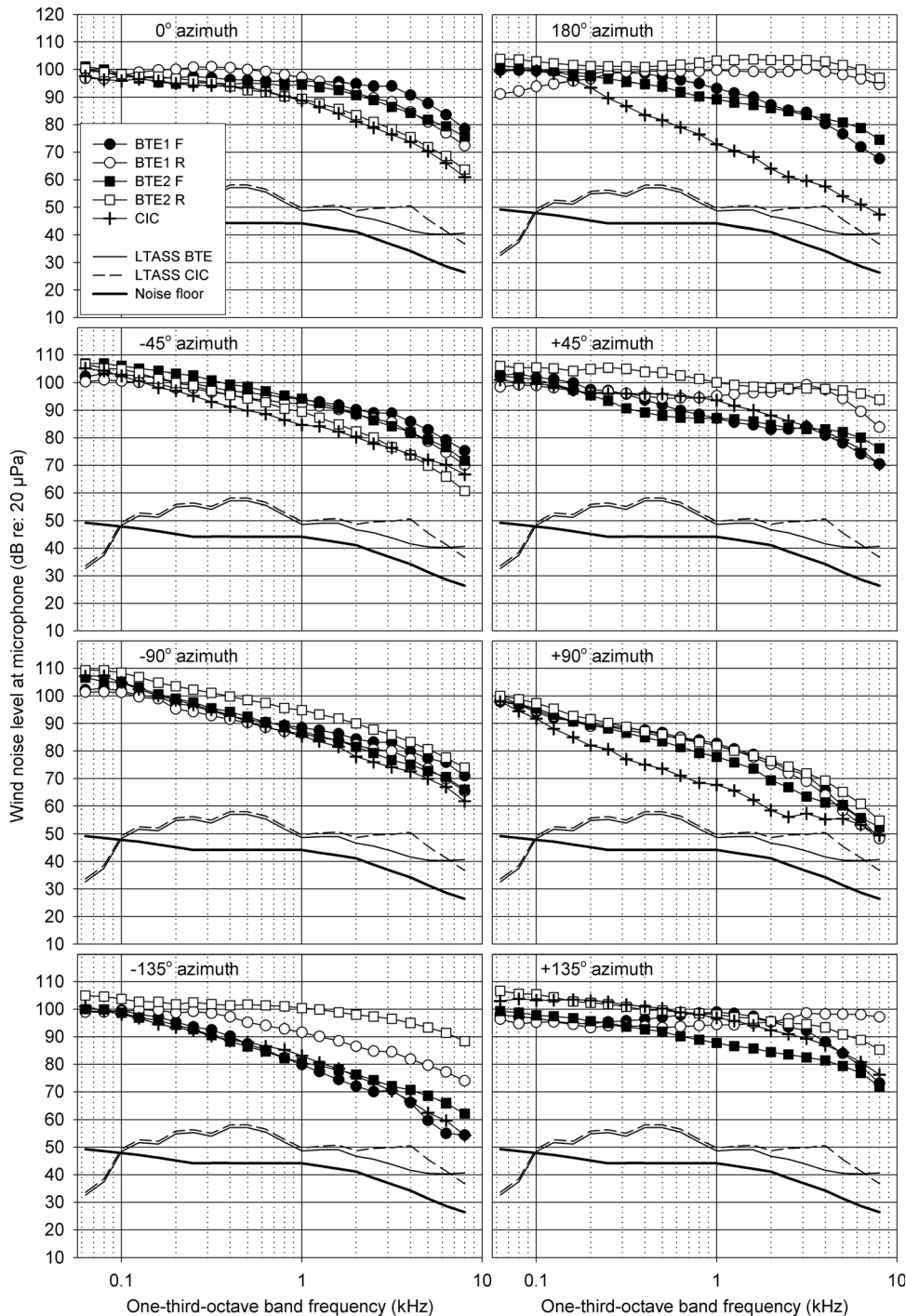


FIG. 6. As for Figure 4, except for a wind speed of 12 m/s.

differences tended to be positive (i.e., BTE2 level higher) at all azimuths (up to 8 dB at 3 m/s) except at  $-45^\circ$  and/or  $0^\circ$  where they were negative (i.e., BTE2 level lower) and as great as  $-6$  dB at 3 m/s. Compared with the front microphone of BTE1, the greatest positive differences for the CIC device (i.e., CIC level greater) were at  $135^\circ$  for all wind speeds (up to 10 dB at 3 m/s), while the greatest negative differences (i.e., CIC level lower) tended to be at  $90^\circ$ ,  $180^\circ$ ,  $-45^\circ$ , or  $0^\circ$  (as great as  $-10$  dB at 3 m/s).

#### IV. DISCUSSION

Some previous studies of wind-noise at the hearing-aid input used wind speeds of 2.1 and/or 5 m/s (Dillon *et al.*,

1999, 2000; Beard and Nepomuceno, 2001; Thompson and Dillon, 2002), while Chung *et al.* (2009, 2010) mainly used speeds of 4.5, 9.0 and 13.5 m/s, and the current study used speeds of 3, 6, and 12 m/s. Therefore, comparisons with previous studies cannot be made at identical wind speeds. For the current study, logarithmic spacing of wind speeds was chosen because a simple theoretical analysis showed that for low-turbulence air flows, the rms sound pressure in a band is proportional to the square of the flow speed (Strasberg, 1988). This translates to a 12-dB increase in sound pressure level for each doubling of flow speed. Other factors, such as a more turbulent air flow (Morgan and Raspert, 1992), can lead to greater growth of wind-noise level with increasing

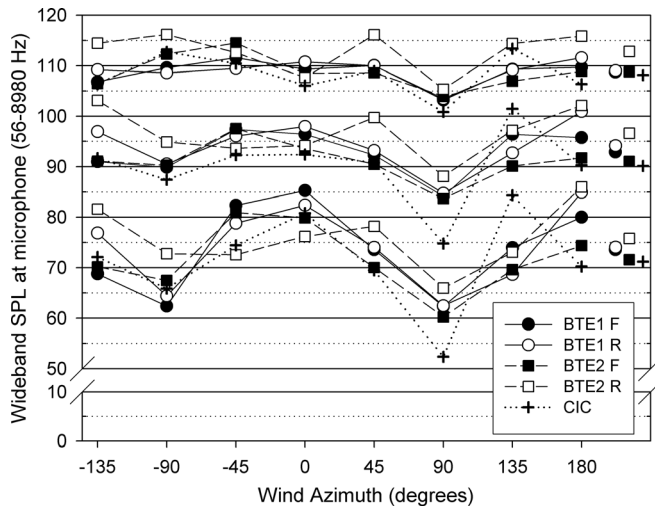


FIG. 7. Wideband wind-noise levels for 3 m/s (lower plots), 6 m/s (middle plots), and 12 m/s (upper plots). The symbols to the right of the 180° point show the average across azimuths.

wind speed. The current study showed differences in overall and one-third-octave band wind-noise levels of more and less than 12 dB between wind speeds of 3 and 6 m/s (below microphone saturation).

Another difference across studies is the measurement duration, which where specified varies from 9 s (current study) to 16 s (Grenner *et al.*, 2000) to 30 s (Chung *et al.*, 2009, 2010). For long-term-average measurements, long durations could better capture any very slow variations of turbulence generated by the head or inherent in a non-laminar, generated wind stream. Since the latter would depend on the stability and characteristics of individual wind generators, its effect on the minimum required measurement duration would differ across studies. Without repeated measurements to quantify variability, the consistency of the trends shown in Figures 7 and 8 suggests that the 9 s measurement duration was not grossly inadequate with the experimental apparatus used for the current study. This averaging time is sufficient to capture wind-noise level variations faster than 0.11 Hz.

A third difference across studies was the wind azimuths, which were 0–360° in 45° steps for the current study compared with 0° only (Grenner *et al.*, 2000), the frontal arc from –90° to +90° in 10° steps (Dillon *et al.*, 1999; 2000; Thompson and Dillon, 2002), and 0–360° in 10° steps (Beard and Nepomuceno, 2001; Chung *et al.*, 2009, 2010). Thus, compared with previous studies that also covered a 360° arc of azimuths, the current study’s more widely spaced azimuths either matched or differed by half of a 10° step. It was thought that 45° steps would allow a fundamental understanding of whether front-versus-rear microphone levels vary with azimuth across devices, would be easily understood by hearing-aid users, and allowed a more detailed spectral understanding of how wind-noise levels compare with speech and vary between microphones within and across devices.

With the aforementioned differences between studies in mind, the 6 m/s, front-microphone, wideband levels of the

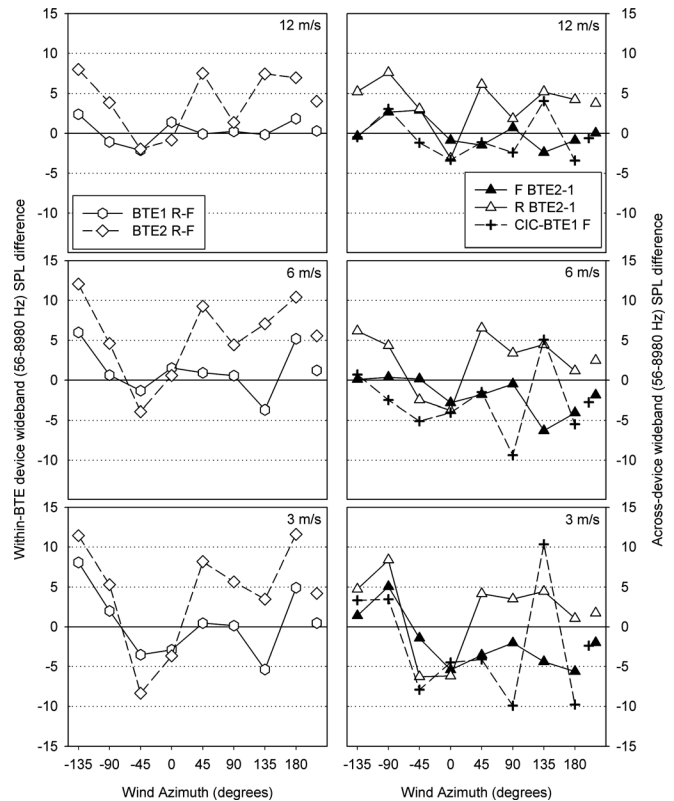


FIG. 8. The wideband wind-noise level at the rear microphone relative to the front microphone for each BTE device (left graphs), and at each microphone of BTE2 and the CIC device relative to the equivalent (i.e., front or rear) microphone of BTE1 (right graphs). Data are shown for wind speeds of 3 m/s (bottom graphs), 6 m/s (middle graphs), and 12 m/s (top graphs). The symbols to the right of the 180° point show the average across azimuths.

current study generally fit between the 4.5 and 9 m/s omnidirectional data of Chung *et al.* (2009, 2010) for wind from the front and rear, but are generally higher than the 9 m/s data for wind from either side. As for the current study, Thompson and Dillon (2002) directly measured the microphone output, and compared with their one-third-octave band spectra for wind at 5 m/s, the current study’s 6 m/s spectra are lower for wind from in front but are generally comparable for wind from either side. Thus, the 6 m/s data from the current study tend to broadly agree with comparable data from previous studies at some azimuths and differ at others. The current and previous studies have shown that large differences in wind-noise levels are possible between devices of the same hearing-aid style (Thompson and Dillon, 2002; Chung *et al.*, 2009), or within the same device if a wind screen is added (Grenner *et al.*, 2000). Thus, differences between studies could be attributable to differences in microphone location, wind shielding, experimental apparatus and/or methods, or measurement and/or analysis bandwidth.

Microphone output signal saturation was achieved at 12 m/s, which is 43 km/h, 27 mph, 23 knots, and rating 6 (i.e., a strong breeze, less than gale force) on the 13-point Beaufort wind force scale. The flattening of the wind-noise spectra at 12 m/s could have been at least partly due to the generation

of clipping harmonics. Clipping would also result in the distortion of speech or other sounds embedded in the wind noise, and potentially reduce sound quality and hence satisfaction with hearing aids. The microphone output signal was approximately 0.8 volts peak-to-peak at saturation, so wind noise also has the potential to saturate 1 volt pre-amplifier and analog-to-digital converter circuits at 12 m/s or lower wind speeds, such as 6 m/s, with sufficient pre-amplifier gain. Conversely, clipping could be avoided at 12 m/s if a suitable wind screen reduced wind-noise levels at the microphone input (Grenner *et al.*, 2000) and the pre-amplifier gain was reduced to 0 dB in wind. Future research could investigate the potential of different wind screen designs to avoid saturation at the hearing-aid input.

Wideband wind-noise levels tended to be higher at the rear than the front microphones of the BTE devices, although this varied with azimuth (see Figure 8, left graphs). The smaller range of differences at 12 m/s may have been at least partly due to the saturation of both microphones. At 3 and 6 m/s, the combined effects of differences in BTE shell size, wind shielding, and microphone location were more clearly seen. These factors cannot be separated with the current data and would be an interesting topic for future research, although their effects may be postulated as follows. Microphone location was probably a factor since obstacles such as the head and pinna can act as wind guards or turbulence sources depending on the azimuth, and turbulence velocity varies around the pinna (Dillon *et al.*, 2000). The magnitude of the rear-minus-front differences tended to be smaller for BTE1, and this may have been due its microphone ports sitting higher above the pinna than those of BTE2 (i.e., reduced localized pinna effects) and not being shielded (i.e., no localized shielding effects). Furthermore, the rearward-facing, half-dome, wind shield over BTE2's rear microphone may have acted as a wind scoop and enhanced wind noise for rearward azimuths.

Compared with BTE1, front-microphone levels tended to be lower for BTE2 and the CIC device, while rear-microphone wind-noise levels tended to be higher for BTE2, although this varied with azimuth (see Figure 8, right graphs). As postulated above, this may have been due to differences in shell size, wind shielding, and microphone location that cannot be separated with the current data, and would be an interesting topic for future research. For wind at 3 m/s from the non-aid side (i.e.,  $-45^\circ$  to  $-135^\circ$ ) and  $0^\circ$ , the similar differences between devices suggest head-generated turbulence had the greatest effect. For wind from the hearing-aid side (i.e.,  $45^\circ$  to  $135^\circ$ ) and  $180^\circ$ , the generally negative BTE front-microphone differences (i.e., BTE2 levels lower) and positive BTE rear-microphone differences (i.e., BTE2 levels greater) suggest the pinna and/or wind shields had a larger effect. Since the CIC and BTE1 microphones did not have wind shields, differences between them were probably due to differences in microphone placement relative to the pinna and turbulence generated by BTE1's shell. For example, the pinna may have shielded the CIC device's microphone at  $180^\circ$  and directed turbulence generated by its ridges into the concha at  $135^\circ$ , while at  $90^\circ$  the concha may have filled with a protective layer of still air.

Wind-noise levels tended to be greater than the LTASS (talker at  $0^\circ$ ) in the lower frequencies at 3 m/s, at most frequencies at 6 m/s, and at all frequencies at 12 m/s where wideband speech-to-wind-noise ratios were in the vicinity of  $-45$  dB. At the lower wind speeds, upward spread of simultaneous masking (Egan and Hake, 1950) that tends to increase with sensorineural hearing loss (Jerger *et al.*, 1960; Florentine *et al.*, 1980; Tyler *et al.*, 1983; Glasberg and Moore, 1986) could cause low-frequency wind noise to mask important middle- and high-frequency speech information. The extent of this effect would depend on the individual hearing loss, the aid's gain-frequency response, and the intrusion of wind into the ear canal via the ear mold vent. The speech-to-wind-noise ratio could be improved through BTE shell design and/or with wind screens that attenuate wind noise more than speech (Grenner *et al.*, 2000). Future research could investigate speech understanding in wind noise and the effects of microphone placement, wind screen, wind shield, and hearing-aid shell design on the speech and wind-noise spectra at the hearing-aid input.

Engineering considerations for improving satisfaction in wind noise can be divided into: (1) Mechanical design to maximize the acoustic signal-to-wind-noise ratio at the hearing-aid input; and (2) Appropriate signal processing for wind noise. Mechanical design includes consideration of pinna effects regarding microphone placement, turbulence generated by the hearing-aid shell, and the effects of wind screens and wind shields. Signal processing includes minimizing pre-amplifier gain in wind to avoid clipping distortion, and adaptive algorithms that better deal with wind noise. For example, previous studies have shown that switching from a directional to an omni-directional microphone in wind would reduce the wind-noise level at the hearing-aid input (Beard and Nepomuceno, 2001; Thompson and Dillon, 2002; Chung *et al.*, 2009, 2010). The current study shows that automatic selection of the omni-directional microphone with the least wind noise could reduce wind-noise levels by up to 8 dB (rear microphone lower) or 12 dB (front microphone lower) depending on azimuth (see Figure 8, left graphs) compared with a BTE device that always switches to the same omni-directional microphone in wind. At wind speeds where at least one microphone is not in saturation, audio could be streamed wirelessly from the ear with less wind noise to the other ear when a loss of binaural cues is less important than reducing wind noise.

Audiological selection of hearing aids that are more likely to be satisfactory in wind noise is not straightforward. Previous studies on wind noise at the hearing-aid input have not been unanimous regarding hearing-aid style. The current study suggests CIC devices are preferable to BTE devices on average, except most notably at  $135^\circ$  where turbulence in the concha increased markedly. However, other styles of in-ear aid were not evaluated. Dillon *et al.* (1999, 2000) recommended against fitting BTE devices because the microphone was usually in the wake of the pinna, which often resulted in greater wind-noise levels than with their ITE, ITC, and CIC devices. In contrast, Chung *et al.* (2010) recommended BTE aids for outdoor activities since their BTE aid had lower or comparable wind-noise levels than their in-ear aids over a wide range of azimuths, and another BTE aid had a similar

pattern of results (Chung *et al.*, 2009). Chung *et al.* (2010) also suggested that CIC aids might be preferable to ITE and ITC aids in environments with low wind speeds (approximately 4.5 m/s), where their CIC aid had lower wind-noise levels over a large range of azimuths. However, Thompson and Dillon (2002) found large differences in wind-noise levels between two ITE devices, and suggested this may have been due to physical differences between the devices and/or measurement facilities.

While in-ear styles of hearing aid may be more or less affected by wind noise than BTE aids in different situations, they are generally not suitable for more severe hearing loss, and signal processing for wind noise is likely to differ across manufacturers. Aid users should be counseled that wind noise is minimized at around 90° azimuth (i.e., wind into the aided ear) for monaural fittings, and 135° should probably be avoided with a CIC device. With binaural fittings, each aid is exposed to a different wind azimuth, and the current study shows one-third-octave, wind-noise spectra for binaural left/right ear pairs; apart from the top row, each row of graphs in Figs. 4–6 can be interpreted to show the azimuth relative to the left ear (left graph) and right ear (right graph) for a single wind direction. These data suggest that the binaural wind-noise level would be minimized with one ear facing into the wind (90°) and the other ear facing away from the wind (–90°).

Satisfaction with hearing aids in wind noise lags behind satisfaction in other areas, and overall satisfaction with hearing-aid benefit increases with the percentage of satisfactory listening situations (Kochkin, 2010). Increased satisfaction may in turn lead to greater hearing-aid usage and fewer returns. Satisfaction in wind noise could be improved with future research into areas such as (1) the efficacy of different wind shield and wind screen designs; (2) the effect of hair, clothing, and the torso (as opposed to a bald KEMAR head) on wind noise; (3) the effect of ear-mold venting on wind noise levels in the ear canal; (4) speech recognition and understanding at different wind speeds; (5) factors that affect the ability of algorithms to detect wind; and (6) the effect of signal processing algorithms on speech understanding and listening comfort in wind noise.

## V. CONCLUSIONS

One-third-octave, wind-noise levels at the front and rear microphones of two BTE devices and the microphone of one CIC device were greater than 65 dB SPL speech levels in all one-third-octave bands for a wind speed of 12 m/s, most bands at 6 m/s, and in the lower speech frequencies for 3 m/s. Wind-noise levels varied with wind speed, wind azimuth, ear-level device, and microphone within each BTE device. Wideband level differences were up to 12 dB between microphones within the same BTE device, and between BTE devices differences were up to 6 dB (front microphones) or 8 dB (rear microphones). Averaged across azimuths, wind-noise levels were lowest at the CIC device's microphone, approximately 1 dB higher at the front microphone of BTE2, and highest at the rear microphone of BTE2. The microphones were saturated at 12 m/s and resulted in wideband wind-noise levels of up to 116 dB SPL at the hearing-aid input.

## ACKNOWLEDGMENTS

The author would like to thank Dr. George Raicevich and Professor Harvey Dillon (The National Acoustic Laboratories, Sydney, Australia) for their advice regarding the wind generator and KEMAR head used in this study, Frauke Schall for her contributions to a lead-up study, and Dr. Dominic Godwin for suggesting possible publication of the data.

- Beard, J., and Nepomuceno, H. (2001). "Wind noise levels for an ITE hearing aid," Knowles Electronics Engineering Report No. 128, revision A, Itasca, IL.
- Burkhard, M. D., and Sachs, R. M. (1975). "Anthropometric manikin for acoustic research," *J. Acoust. Soc. Am.* **58**, 214–222.
- Byrne, D. Dillon, H. Tran, K. Arlinger, S. Wilbraham, K. Cox, R. Hagerman, B. Hetu, R. Kei, J. Lui, C. Kiessling, J. Kotby, M. N. Nasser, N. H. A. El Kholly, W. A. H. Nakanishi, Y. Oyer, H. Powell, R. Stephens, D. Meredith, R. Sirimanna, T. Tavartkiladze, G. Frolov, G. I. Westerman, S., and Ludvigsen, C. (1994). "An international comparison of long-term average speech spectra," *J. Acoust. Soc. Am.* **96**, 2108–2120.
- Chung, K. (2004). "Challenges and recent developments in hearing aids. Part I. Speech understanding in noise, microphone technologies and noise reduction algorithms," *Trends Amplif.* **8**, 83–124.
- Chung, K. Mongeau, L., and McKibben, N. (2009). "Wind noise in hearing aids with directional and omnidirectional microphones: Polar characteristics of behind-the-ear hearing aids," *J. Acoust. Soc. Am.* **125**, 2243–2259.
- Chung, K. McKibben, N., and Mongeau, L. (2010). "Wind noise in hearing aids with directional and omnidirectional microphones: Polar characteristics of custom-made hearing aids," *J. Acoust. Soc. Am.* **127**, 2529–2542.
- Dillon, H. (2001). "Electroacoustic performance and measurement." in *Hearing Aids*. First edition, Sydney: Boomerang, pg. 93.
- Dillon, H. Katsch, R., and Roe, I. (1999). "Wind noise in hearing aids," presented at *Hearing Aid Amplification for the New Millennium*, Sydney, Australia. [http://www.nal.gov.au/pdf/wind noise.ppt](http://www.nal.gov.au/pdf/wind%20noise.ppt) (Last viewed 27 April 2011).
- Dillon, H. Roe, I., and Katsch, R. (2000). "The sources of wind noise in hearing aids," poster presented at *The International Hearing Aid Research Conference*, Lake Tahoe, CA. [http://www.nal.gov.au/pdf/Wind noise causes poster.ppt](http://www.nal.gov.au/pdf/Wind%20noise%20causes%20poster.ppt) (Last viewed 27 April 2011).
- Egan, J. P., and Hake, H. W. (1950). "On the masking pattern of a simple auditory stimulus," *J. Acoust. Soc. Am.* **22**, 622–630.
- Fishburn, M., Colin-Thome, G., and Always, P. (2007). "Generating a 'silent' flow of air to measure the aerodynamic and acoustical performance of a louvre under acoustical laboratory conditions," the 14th International Congress on Sound and Vibration, Cairns, Australia, 9–12 July.
- Florentine, M., Buus, S., Scharf, B., and Zwicker, E. (1980). "Frequency selectivity in normally-hearing and hearing-impaired observers," *J. Speech Hearing Res.* **23**, 646–669.
- Glasberg, B. R., and Moore, B. C. J. (1986). "Auditory filter shapes in subjects with unilateral and bilateral cochlear impairments," *J. Acoust. Soc. Am.* **79**, 1020–1033.
- Grenner, J., Abrahamsson, U., Jernberg, B., and Lindblad, S. (2000). "A comparison of wind noise in four hearing instruments," *Scand. Audiol.* **29**, 171–174.
- Jerger, J. F. Tillman, T. W. and Peterson, J. L. (1960). "Masking by octave bands of noises in normal and impaired ears," *J. Acoust. Soc. Am.* **32**, 385–390.
- Kochkin, S. (2010). "MarkeTrak VIII: Consumer satisfaction with hearing aids is slowly increasing," *Hearing J.* **63**(1), 19–32.
- Morgan, S., and Raspert, R. (1992). "Investigation of the mechanisms of low-frequency wind noise generation outdoors," *J. Acoust. Soc. Am.* **92**, 1180–1183.
- Strasberg, M. (1988). "Dimensional analysis of windscreen noise," *J. Acoust. Soc. Am.* **83**, 544–548.
- Thompson, S., and Dillon, H. (2002). "Recent studies on wind noise in hearing aids," presented at the American Academy of Audiology Convention, Philadelphia, PA. [http://www.nal.gov.au/pdf/Thompson and Dillon 2002 Recent Studies on Wind Noise in Hearing Aids AAA Convention.pdf](http://www.nal.gov.au/pdf/Thompson%20and%20Dillon%202002%20Recent%20Studies%20on%20Wind%20Noise%20in%20Hearing%20Aids%20AAA%20Convention.pdf) (Last viewed 27 April 2011).
- Tyler, R. S. Wood, E. J. and Fernandes, M. (1983). "Frequency resolution and discrimination of constant and dynamic tones in normal and hearing-impaired listeners," *J. Acoust. Soc. Am.* **74**, 1190–1199.